5 - EFDC SEDIMENT PROCESS MODEL

A sediment process model developed by DiToro and Fitzpatrick (1993; hereinafter referred to as D&F) and was coupled with CE-QUAL-ICM for Chesapeake Bay water quality modeling (Cerco and Cole 1993). The sediment process model was slightly modified and incorporated into the EFDC water quality model to simulate the processes in the sediment and at the sediment-water interface. The description of the EFDC sediment process model in this section is from Park et al. (1995). The sediment process model has 27 water-quality related state variables and fluxes (Table 5-1).

Table 5-1. EFDC sediment process model state variables and flux terms

(1) particulate organic carbon G1 class in layer 2	(15) nitrate nitrogen in layer 1
(2) particulate organic carbon G2 class in layer 2	(16) nitrate nitrogen in layer 2
(3) particulate organic carbon G3 class in layer 2	(17) phosphate phosphorus in layer 1
(4) particulate organic nitrogen G1 class in layer 2	(18) phosphate phosphorus in layer 2
(5) particulate organic nitrogen G2 class in layer 2	(19) available silica in layer 1
(6) particulate organic nitrogen G3 class in layer 2	(20) available silica in layer 2
(7) particulate organic phosphorus G1 class in layer 2	(21) ammonia nitrogen flux
(8) particulate organic phosphorus G2 class in layer 2	(22) nitrate nitrogen flux
(9) particulate organic phosphorus G3 class in layer 2	(23) phosphate phosphorus flux
(10) particulate biogenic silica in layer 2	(24) silica flux
(11) sulfide/methane in layer 1	(25) sediment oxygen demand
(12) sulfide/methane in layer 2	(26) release of chemical oxygen demand
(13) ammonia nitrogen in layer 1	(27) sediment temperature
(14) ammonia nitrogen in layer 2	

The nitrate state variables, (15), (16), and (22), in the model represent the sum of nitrate and nitrite nitrogen. The three G classes for particulate organic matter (POM) in Layer 2 and the two layers for inorganic substances are described below.

In the sediment model, benthic sediments are represented as two layers (Fig. 5-1). The upper layer (Layer 1) is in contact with the water column and may be oxic or anoxic depending on dissolved oxygen concentration in the overlying water. The lower layer (Layer 2) is permanently anoxic. The upper layer depth, which is determined by the penetration of oxygen into the sediments, is at its maximum only a small fraction of the total depth. Because H_1 (~ 0.1 cm) « H_2,

$$H = H_1 + H_2 \approx H_2 \tag{5-1}$$

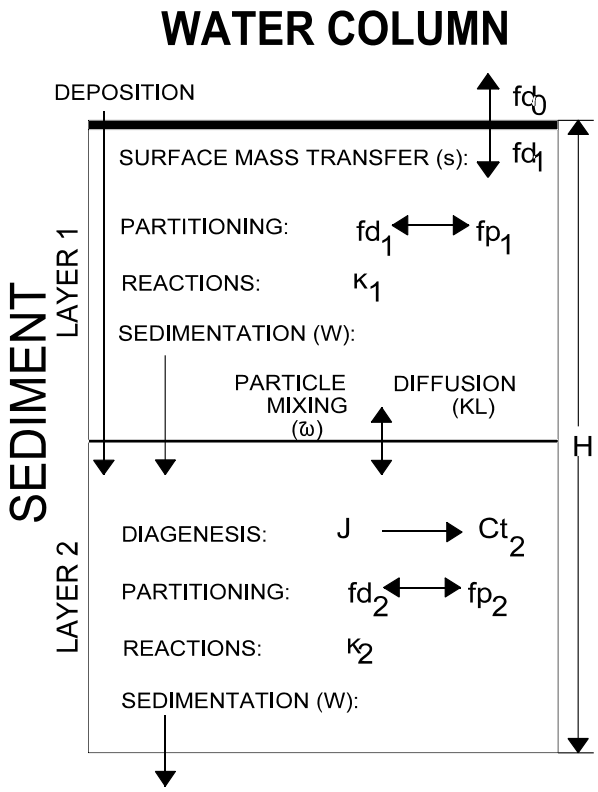

Figure 5-1. Sediment layers and processes included in sediment process model.

where H is the total depth (approximately 10 cm), H_1 is the upper layer depth and H_2 is the lower layer depth.

The model incorporates three basic processes (Fig. 5-2): (1) depositional flux of POM, (2) the diagenesis of POM, and (3) the resulting sediment flux. The sediment model is driven by net settling of particulate organic carbon, nitrogen, phosphorus, and silica from the overlying water to the sediments (**depositional flux**). Because of the negligible thickness of the upper layer (Eq. 5-1), deposition is considered to proceed from the water column directly to the lower layer. Within the lower layer, the model simulates the diagenesis (mineralization or decay) of deposited POM, which produces oxygen demand and inorganic nutrients (**diagenesis flux**). The third basic process is the flux of substances produced by diagenesis (**sediment flux**). Oxygen demand, as sulfide (in salt water) or methane (in fresh water), takes three paths out of the sediments: (1) oxidation at the sediment-water interface as sediment oxygen demand, (2) export to the water column as chemical oxygen demand, or (3) burial to deep, inactive

sediments. Inorganic nutrients produced by diagenesis take two paths out of the sediments: (1) release to the water column or (2) burial to deep, inactive sediments (Fig. 5-2).

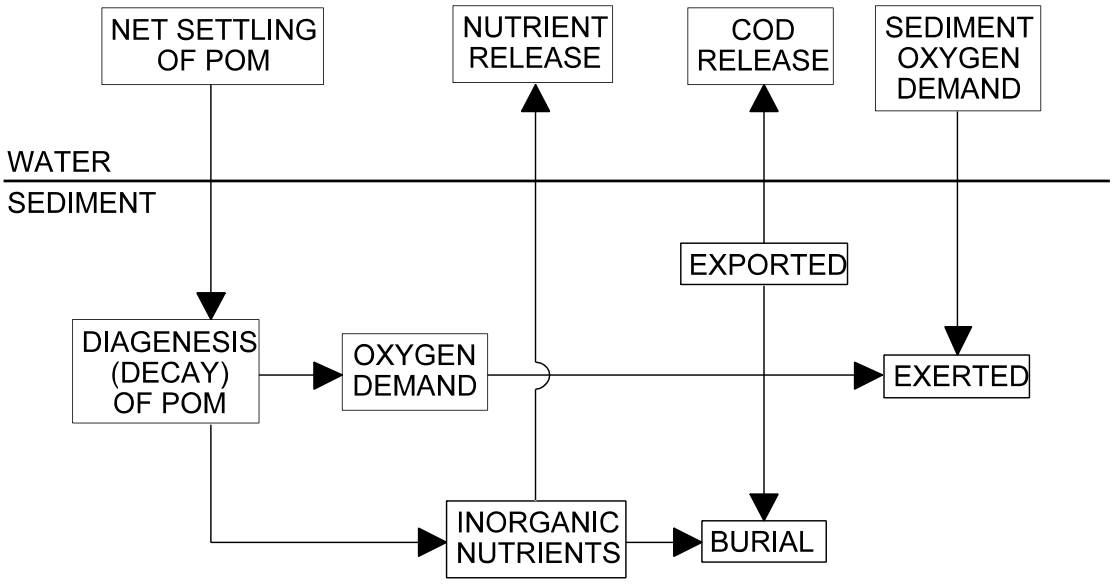

Figure 5-2. Schematic diagram for sediment process model

This section describes the three basic processes with reactions and sources/sinks for each state variable. The method of solution includes finite difference equations, solution scheme, boundary, and initial conditions. Complete model documentation can be found in D&F (1993).

5.1 Depositional Flux

Deposition is one process that couples the water column model with the sediment model. Consequently, deposition is represented in both the water column and sediment models. In the water column model, the governing mass-balance equations for the following state variables contain settling terms, which represent the depositional fluxes:

- three algal groups, cyanobacteria, diatoms and green algae (Eq. 4-5)
- refractory and labile particulate organic carbon (Equations 4-20 and 4-21)
- refractory and labile particulate organic phosphorus (Equations 4-35 and 4-36) and total phosphate (Eq. 4-38)
- refractory and labile particulate organic nitrogen (Equations 4-48 and 4-49)
- particulate biogenic silica (Eq. 4-61) and available silica (Eq. 4-62).

The sediment model receives these depositional fluxes of particulate organic carbon (POC), particulate organic nitrogen (PON), particulate organic phosphorus (POP), and particulate biogenic silica (PSi). Because of the negligible thickness of the upper layer (Eq. 5-1), deposition is considered to proceed from the water column directly to the lower layer. Since the sediment model has three G classes of POM, G_i (i = 1, 2, or 3), depending on the time scales of reactivity (Section 5.2), the POM fluxes from the water column should be mapped into three G classes based on their reactivity. Then the depositional fluxes for the ith G class (i = 1, 2, or 3) may be expressed as:

$$J_{POC,i} = FCLP_i \cdot WS_{LP} \cdot LPOC^N + FCRP_i \cdot WS_{RP} \cdot RPOC^N + \sum_{x=c,d,g} FCB_{x,i} \cdot WS_x \cdot B_x^N \quad (5\text{-}2)$$

$$J_{PON,i} = FNLP_i \cdot WS_{LP} \cdot LPON^N + FNRP_i \cdot WS_{RP} \cdot RPON^N + \sum_{x=c,d,g} FNB_{x,i} \cdot ANC_x \cdot WS_x \cdot B_x^N \quad (5\text{-}3)$$

$$J_{POP,i} = FPLP_i \cdot WS_{LP} \cdot LPOP^N + FPRP_i \cdot WS_{RP} \cdot RPOP^N + \sum_{x=c,d,g} FPB_{x,i} \cdot APC \cdot WS_x \cdot B_x^N + \gamma_i \cdot WS_{TSS} \cdot PO4p^N \quad (5\text{-}4)$$

$$J_{PSi} = WS_d \cdot SU^N + ASC_d \cdot WS_d \cdot B_d^N + WS_{TSS} \cdot SAp^N \quad (5\text{-}5)$$

$J_{POM,i}$ = depositional flux of POM (M = C, N or P) routed into the i^{th} G class (g m^{-2} day^{-1})

J_{PSi} = depositional flux of PSi (g Si m^{-2} day^{-1})

$FCLP_i$, $FNLP_i$, $FPLP_i$ = fraction of water column labile POC, PON, and POP, respectively, routed into the i^{th} G class in sediment

$FCRP_i$, $FNRP_i$, $FPRP_i$ = fraction of water column refractory POC, PON, and POP, respectively, routed into the i^{th} G class in sediment

$FCB_{x,i}$, $FNB_{x,i}$, $FPB_{x,i}$ = fraction of POC, PON, and POP, respectively, in the algal group x routed into the i^{th} G class in sediment

γ_i = 1 for i = 1
0 for i = 2 or 3.

In the source code, the sediment process model is solved after the water column water quality model, and the calculated fluxes using the water column conditions at $t = t_n$ are used for the computation of the water quality variables at $t = t_n + \theta$. The superscript N indicates the variables after being updated for the kinetic processes, as defined in Eq. 4-82.

The settling of sorbed phosphate is considered to contribute to the labile G_1 pool in Eq. 5-4, and settling of sorbed silica contributes to J_{PSi} in Eq. 5-5 to avoid creation of additional depositional fluxes for

inorganic particulates. The sum of distribution coefficients should be unity: $\sum_i FCLP_i = \sum_i FNLP_i = \sum_i FPLP_i = \sum_i FCRP_i = \sum_i FNRP_i = \sum_i FPRP_i = \sum_i FCB_{x,i} = \sum_i FNB_{x,i} = \sum_i FPB_{x,i} = 1$. The settling velocities, WS_{LP}, WS_{RP}, WS_x, and WS_{TSS}, as defined in the EFDC water column model (Section 4), are net settling velocities. If total active metal is selected as a measure of sorption site, WS_{TSS} is replaced by WS_s in Equations 5-4 and 5-5 (see Sections 4.5 and 4.7).

5.2 Diagenesis Flux

Another coupling point of the sediment model to the water column model is the sediment flux, which is described in Section 5.3. The computation of sediment flux requires that the magnitude of the diagenesis flux be known. The diagenesis flux is explicitly computed using mass-balance equations for deposited POC, PON, and POP. (Dissolved silica is produced in the sediments as the result of the dissolution of PSi. Since the dissolution process is different from the bacterial-mediated diagenesis process, it is presented separately in Section 5.4.) In the mass-balance equations, the depositional fluxes of POM are the source terms and the decay of POM in the sediments produces the diagenesis fluxes. The integration of the mass-balance equations for POM provides the diagenesis fluxes that are the inputs for the mass-balance equations for ammonium, nitrate, phosphate, and sulfide/methane in the sediments (Section 5.3).

The difference in decay rates of POM is accounted for by assigning a fraction of POM to various decay classes (Westrisch and Berner 1984). POM in the sediments is divided into three G classes, or fractions, representing three scales of reactivity. The G_1 (labile) fraction has a half life of 20 days, and the G_2 (refractory) fraction has a half life of one year. The G_3 (inert) fraction is nonreactive, i.e., it undergoes no significant decay before burial into deep, inactive sediments. The varying reactivity of the G classes controls the time scale over which changes in depositional flux will be reflected in changes in diagenesis flux. If the G_1 class would dominate the POM input into the sediments, then there would be no significant time lag introduced by POM diagenesis and any changes in depositional flux would be readily reflected in diagenesis flux.

Because the upper layer thickness is negligible (Eq. 5-1) and thus depositional flux is considered to proceed directly to the lower layer (Equations 5-2 to 5-5), diagenesis is considered to occur in the lower layer only. The mass-balance equations are similar for POC, PON, and POP, and for different G classes. The mass-balance equation in the anoxic lower layer for the i^{th} G class (i = 1, 2, or 3) may be expressed as:

$$H_2 \frac{\partial G_{POM,i}}{\partial t} = - K_{POM,i} \cdot \theta_{POM,i}^{T-20} \cdot G_{POM,i} \cdot H_2 - W \cdot G_{POM,i} + J_{POM,i} \qquad (5\text{-}6)$$

$G_{POM,i}$ = concentration of POM (M = C, N, or P) in the i^{th} G class in Layer 2 (g m^{-3})

$K_{POM,i}$ = decay rate of the i^{th} G class POM at 20°C in Layer 2 (day^{-1})

$\theta_{POM,i}$ = constant for temperature adjustment for $K_{POM,i}$

T = sediment temperature (°C)

W = burial rate (m day^{-1}).

Since the G_3 class is inert, $K_{POM,3} = 0$.

Once the mass-balance equations for $G_{POM,1}$ and $G_{POM,2}$ are solved, the diagenesis fluxes are computed from the rate of mineralization of the two reactive G classes:

$$J_M = \sum_{i=1}^{2} K_{POM,i} \cdot \theta_{POM,i}^{T-20} \cdot G_{POM,i} \cdot H_2 \qquad (5\text{-}7)$$

J_M = diagenesis flux (g $^{-2}$ day^{-1}) of carbon (M = C), nitrogen (M = N), or phosphorus (M = P).

5.3 Sediment Flux

The mineralization of POM produces soluble intermediates, which are quantified as diagenesis fluxes in the previous section. The intermediates react in the oxic and anoxic layers, and portions are returned to the overlying water as sediment fluxes. Computation of sediment fluxes requires mass-balance equations for ammonium, nitrate, phosphate, sulfide/methane, and available silica. This section describes the flux portion for ammonium, nitrate, phosphate, and sulfide/methane of the model. Available silica is described in Section 5.4.

In the upper layer, the processes included in the flux portion are (Fig. 5-1)

- exchange of dissolved fraction between Layer 1 and the overlying water
- exchange of dissolved fraction between Layer 1 and 2 via diffusive transport
- exchange of particulate fraction between Layer 1 and 2 via particle mixing
- loss by burial to the lower layer (Layer 2)
- removal (sink) by reaction
- internal sources.

Since the upper layer is quite thin, H_1 ~ 0.1 cm (Eq. 5-1) and the surface mass transfer coefficient (s) is on the order of 0.1 m day^{-1}, then the residence time in the upper layer is $H_1/s \sim 10^{-2}$ days. Hence, a steady-state approximation is made in the upper layer. Then the mass-balance equation for ammonium, nitrate, phosphate, or sulfide/methane in the upper layer is:

$$H_1 \frac{\partial Ct_1}{\partial t} = 0 = s(fd_0 \cdot Ct_0 - fd_1 \cdot Ct_1) + KL(fd_2 \cdot Ct_2 - fd_1 \cdot Ct_1)$$

$$+ \ \omega(fp_2 \cdot Ct_2 \ - \ fp_1 \cdot Ct_1) \ - \ W \cdot Ct_1 \ - \ \frac{\kappa_1^2}{s} Ct_1 \ + \ J_1 \qquad (5\text{-}8)$$

Ct_1 & Ct_2 = total concentrations in Layer 1 and 2, respectively (g m^{-3})

Ct_o = total concentration in the overlying water (g m^{-3})

s = surface mass transfer coefficient (m day^{-1})

KL = diffusion velocity for dissolved fraction between Layer 1 and 2 (m day^{-1})

ω = particle mixing velocity between Layer 1 and 2 (m day^{-1})

fd_o = dissolved fraction of total substance in the overlying water ($0 \le fd_o \le 1$)

fd_1 = dissolved fraction of total substance in Layer 1 ($0 \le fd_1 \le 1$)

fp_1 = particulate fraction of total substance in Layer 1 ($= 1 - fd_1$)

fd_2 = dissolved fraction of total substance in Layer 2 ($0 \le fd_2 \le 1$)

fp_2 = particulate fraction of total substance in Layer 2 ($= 1 - fd_2$)

κ_1 = reaction velocity in Layer 1 (m day^{-1})

J_1 = sum of all internal sources in Layer 1 (g m^{-2} day^{-1}).

The first term on the RHS of Eq. 5-8 represents the exchange across sediment-water interface. Then the sediment flux from Layer 1 to the overlying water, which couples the sediment model to the water column model, may be expressed as:

$$J_{aq} \ = \ s(fd_1 \cdot Ct_1 \ - \ fd_o \cdot Ct_o) \qquad (5\text{-}9)$$

J_{aq} = sediment flux of ammonium, nitrate, phosphate, or sulfide/methane to the overlying water (g m^{-2} day^{-1}).

The convention used in Eq. 5-9 is that positive flux is from the sediment to the overlying water.

In the lower layer, the processes included in the flux portion are (Fig. 5-1)

- exchange of dissolved fraction between Layer 1 and 2 via diffusive transport
- exchange of particulate fraction between Layer 1 and 2 via particle mixing
- deposition from Layer 1 and burial to the deep inactive sediments
- removal (sink) by reaction
- internal sources including diagenetic source.

The mass-balance equation for ammonium, nitrate, phosphate or sulfide/methane in the lower layer is:

$$H_2 \frac{\partial Ct_2}{\partial t} \ = \ - \ KL(fd_2 \cdot Ct_2 \ - \ fd_1 \cdot Ct_1) \ - \ \omega(fp_2 \cdot Ct_2 \ - \ fp_1 \cdot Ct_1)$$

$$+ \ W(Ct_1 \ - \ Ct_2) \ - \ \kappa_2 \cdot Ct_2 \ + \ J_2 \qquad (5\text{-}10)$$

κ_2 = reaction velocity in Layer 2 (m day^{-1})

J_2 = sum of all internal sources including diagenesis in Layer 2 (g m^{-2} day^{-1}).

The substances produced by mineralization of POM in sediments may be present in both dissolved and particulate phases. This distribution directly affects the magnitude of the substance that is returned to the overlying water. In Equations 5-8 to 5-10, the distribution of a substance between the dissolved and particulate phases in a sediment is parameterized using a linear partitioning coefficient. The dissolved and particulate fractions are computed from the partitioning equations:

$$fd_1 = \frac{1}{1 + m_1 \cdot \pi_1} \qquad fp_1 = 1 - fd_1 \tag{5-11}$$

$$fd_2 = \frac{1}{1 + m_2 \cdot \pi_2} \qquad fp_2 = 1 - fd_2 \tag{5-12}$$

m_1, m_2 = solid concentrations in Layer 1 and 2, respectively (kg L^{-1})

π_1, π_2 = partition coefficients in Layer 1 and 2, respectively (per kg L^{-1}).

The partition coefficient is the ratio of particulate to dissolved fraction per unit solid concentration (i.e., per unit sorption site available).

All terms, except the last two terms, in Equations 5-8 and 5-10 are common to all state variables and are described in Section 5.3.1. The last two terms represent the reaction and source/sink terms, respectively. These terms, which take different mathematical formulations for different state variables, are described in Sections 5.3.2 to 5.3.5 for ammonium, nitrate, phosphate, and sulfide/methane, respectively.

5.3.1 Common Parameters for Sediment Flux

Parameters that are needed for the sediment fluxes are *s*, ϖ, KL, W, H_2, m_1, m_2, π_1, π_2, κ_1, κ_2, J_1, and J_2 in Equations 5-8 to 5-12. Of these, κ_1, κ_2, J_1, and J_2 are variable-specific. Among the other common parameters, W, H_2, m_1, and m_2, are specified as input. The modeling of the remaining three parameters, *s*, ϖ, and KL, is described in this section.

5.3.1.1 Surface mass transfer coefficient. Owing to the observation that the surface mass transfer coefficient, *s*, can be related to the sediment oxygen demand, SOD (DiToro et al. 1990), *s* can be estimated from the ratio of SOD and overlying water oxygen concentration:

$$s = \frac{D_1}{H_1} = \frac{SOD}{DO_0} \tag{5-13}$$

D_1 = diffusion coefficient in Layer 1 (m^2 day^{-1}).

Knowing *s*, it is possible to estimate the other model parameters.

5.3.1.2 Particulate phase mixing coefficient. The particle mixing velocity between Layer 1 and 2 is parameterized as:

$$\omega = \frac{D_p \cdot \theta_{Dp}^{T-20}}{H_2} \frac{G_{POC,1}}{G_{POC,R}} \frac{DO_0}{KM_{Dp} + DO_0} \quad (5\text{-}14)$$

D_p = apparent diffusion coefficient for particle mixing (m^2 day^{-1})

θ_{Dp} = constant for temperature adjustment for D_p

$G_{POC,R}$ = reference concentration for $G_{POC,1}$ (g C m^{-3})

KM_{Dp} = particle mixing half-saturation constant for oxygen (g O_2 m^{-3}).

The enhanced mixing of sediment particles by macrobenthos (bioturbation) is quantified by estimating D_p. The particle mixing appears to be proportional to the benthic biomass (Matisoff 1982), which is correlated to the carbon input to the sediment (Robbins et al. 1989). This is parameterized by assuming that benthic biomass is proportional to the available labile carbon, $G_{POC,1}$, and $G_{POC,R}$ is the reference concentration at which the particle mixing velocity is at its nominal value. The Monod-type oxygen dependency accounts for the oxygen dependency of benthic biomass.

It has been observed that a hysteresis exists in the relationship between the bottom water oxygen and benthic biomass. Benthic biomass increases as the summer progresses. However, the occurrence of anoxia/hypoxia reduces the biomass drastically and also imposes stress on benthic activities. After full overturn, the bottom water oxygen increases, but the population does not recover immediately. Hence, the particle mixing velocity, which is proportional to the benthic biomass, does not increase in response to the increased bottom water oxygen. Recovery of benthic biomass following hypoxic events depends on many factors including severity and longevity of hypoxia, constituent species, and salinity (Diaz and Rosenberg 1995).

This phenomenon of reduced benthic activities and hysteresis is parameterized based on the idea of stress that low oxygen imposes on the benthic population. It is analogous to the modeling of the toxic effect of chemicals on organisms (Mancini 1983). A first order differential equation is employed, in which the benthic stress (1) accumulates only when overlying oxygen is below KM_{Dp} and (2) is dissipated at a first order rate (Fig. 5-3a):

$$\frac{\partial ST}{\partial t} = - K_{ST} \cdot ST + \left(1 - \frac{DO_0}{KM_{Dp}}\right) \qquad if \quad DO_0 < KM_{Dp}$$

$$\frac{\partial ST}{\partial t} = - K_{ST} \cdot ST \qquad if \quad DO_0 > KM_{Dp} \tag{5-15}$$

ST = accumulated benthic stress (day)

K_{ST} = first order decay rate for ST (day^{-1}).

The behavior of this formulation can be understood by evaluating the steady-state stresses at two extreme conditions of overlying water oxygen, DO_0:

as $DO_0 = 0$	$K_{ST} \cdot ST = 1$	$f(ST) = (1 - K_{ST} \cdot ST) = 0$
as $DO_0 \geq KM_{Dp}$	$K_{ST} \cdot ST = 0$	$f(ST) = (1 - K_{ST} \cdot ST) = 1$

The dimensionless expression, $f(ST) = 1 - K_{ST} \cdot ST$, appears to be the proper variable to quantify the effect of benthic stress on benthic biomass and thus particle mixing (Fig. 5-3b).

The final formulation for the particle mixing velocity, including the benthic stress, is:

$$\omega = \frac{D_p \cdot \theta_{Dp}^{T-20}}{H_2} \frac{G_{POC,1}}{G_{POC,R}} \frac{DO_0}{KM_{Dp} + DO_0} f(ST) + \frac{Dp_{min}}{H_2} \tag{5-16}$$

Dp_{min} = minimum diffusion coefficient for particle mixing ($m^2\ day^{-1}$).

The reduction in particle mixing due to the benthic stress, f(ST), is estimated by employing the following procedure. The stress, ST, is normally calculated with Eq. 5-15. Once DO_0 drops below a critical concentration, $DO_{ST,c}$, for $NC_{hypoxia}$ consecutive days or more, the calculated stress is not allowed to decrease until t_{MBS} days of $DO_0 > DO_{ST,c}$. That is, only when hypoxic days are longer than critical hypoxia days ($NC_{hypoxia}$), the maximum stress, or minimum $(1 - K_{ST} \cdot ST)$, is retained for a specified period (t_{MBS} days) after DO_0 recovery (Fig. 5-3). No hysteresis occurs if DO_0 does not drop below $DO_{ST,c}$ or if hypoxia lasts less than $NC_{hypoxia}$ days. When applying maximum stress for t_{MBS} days, the subsequent hypoxic days are not included in t_{MBS}. This parameterization of hysteresis essentially assumes seasonal hypoxia, i.e., one or two major hypoxic events during summer, and might be unsuitable for systems with multiple hypoxic events throughout a year.

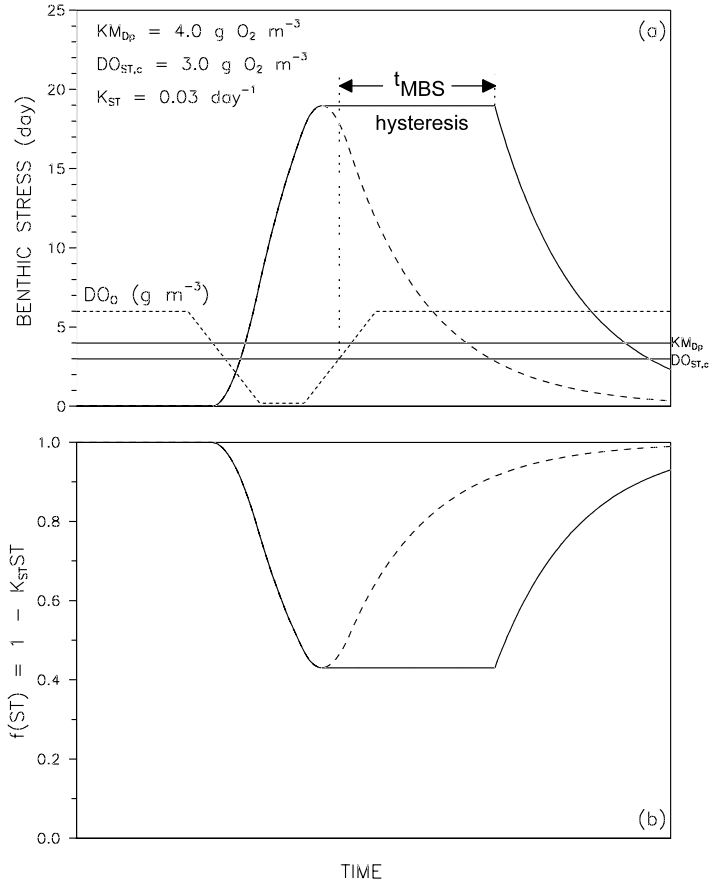

Figure 5-3. Benthic stress (a) and its effect on particle mixing (b) as a function of overlying water column dissolved oxygen concentration

Three parameters relating to hysteresis, $DO_{ST,c}$, $NC_{hypoxia}$, and t_{MBS}, are functions of many factors including severity and longevity of hypoxia, constituent species, and salinity, and thus have site-specific variabilities (Diaz and Rosenberg 1995). The critical overlying oxygen concentration, $DO_{ST,c}$, also depends on the distance from the bottom of the location of $DO_{0.}$ The critical hypoxia days, $NC_{hypoxia}$, depend on tolerance of benthic organisms to hypoxia and thus on benthic community structure (Diaz and Rosenberg 1995). The time lag for the recovery of benthic biomass following hypoxic events, t_{MBS}, tends to be longer for higher salinity. The above three parameters are considered to be spatially constant input parameters.

5.3.1.3 Dissolved phase mixing coefficient. Dissolved phase mixing between Layer 1 and 2 is via passive molecular diffusion, which is enhanced by the mixing activities of the benthic organisms (bio-irrigation). This is modeled by increasing the diffusion coefficient relative to the molecular diffusion coefficient:

$$KL = \frac{D_d \cdot \theta_{Dd}^{T-20}}{H_2} + R_{BI,BT} \cdot \omega \quad (5\text{-}17)$$

D_d = diffusion coefficient in pore water (m^2 day^{-1})

θ_{Dd} = constant for temperature adjustment for D_d

$R_{BI,BT}$ = ratio of bio-irrigation to bioturbation.

The last term in Eq. 5-17 accounts for the enhanced mixing by organism activities.

5.3.2 Ammonia Nitrogen

Diagenesis is assumed not to occur in the upper layer because of its shallow depth, and ammonium is produced by diagenesis in the lower layer:

$$J_{1,NH4} = 0 \qquad J_{2,NH4} = J_N \quad (from\ Eq.\ 5-7) \quad (5\text{-}18)$$

Ammonium is nitrified to nitrate in the presence of oxygen. A Monod-type expression is used for the ammonium and oxygen dependency of the nitrification rate. Then the oxic layer reaction velocity in Eq. 5-8 for ammonium may be expressed as:

$$\kappa_{1,NH4}^2 = \frac{DO_0}{2 \cdot KM_{NH4,O2} + DO_0} \frac{KM_{NH4}}{KM_{NH4} + NH4_1} \kappa_{NH4}^2 \cdot \theta_{NH4}^{T-20} \quad (5\text{-}19)$$

and then the nitrification flux becomes:

$$J_{Nit} = \frac{\kappa_{1,NH4}^2}{s} \cdot NH4_1 \quad (5\text{-}20)$$

$KM_{NH4,O2}$ = nitrification half-saturation constant for dissolved oxygen (g O_2 m^{-3})

$NH4_1$ = total ammonium nitrogen concentration in Layer 1 (g N m^{-3})

KM_{NH4} = nitrification half-saturation constant for ammonium (g N m^{-3})

κ_{NH4} = optimal reaction velocity for nitrification at 20°C (m day^{-1})

θ_{NH4} = constant for temperature adjustment for κ_{NH4}

J_{Nit} = nitrification flux (g N m^{-2} day^{-1}).

Nitrification does not occur in the anoxic lower layer:

$$\kappa_{2,NH4} = 0 \quad (5\text{-}21)$$

Once Equations 5-8 and 5-10 are solved for $NH4_1$ and $NH4_2$, the sediment flux of ammonium to the overlying water, $J_{aq,NH4}$, can be calculated using Eq. 5-9. Note that it is not $NH4_1$ and $NH4_2$ that determine the magnitude of $J_{aq,NH4}$ (Section X-B-2 in D&F 1993). The magnitude is determined by (1) the

diagenesis flux, (2) the fraction that is nitrified, and (3) the surface mass transfer coefficient (*s*) that mixes the remaining portion.

5.3.3 Nitrate Nitrogen

Nitrification flux is the only source of nitrate in the upper layer, and there is no diagenetic source for nitrate in both layers:

$$J_{1,NO3} = J_{Nit} \quad (from\ Eq.\ 5-19) \qquad J_{2,NO3} = 0 \tag{5-22}$$

Nitrate is present in sediments as dissolved substance, i.e., $\pi_{1,NO3} = \pi_{2,NO3} = 0$, making $fd_{1,NO3} = fd_{2,NO3} = 1$ (Equations 5-11 and 5-12): it also makes ϖ meaningless, hence ϖ = 0. Nitrate is removed by denitrification in both oxic and anoxic layers with the carbon required for denitrification supplied by carbon diagenesis. The reaction velocities in Equations 5-8 and 5-10 for nitrate may be expressed as:

$$\kappa^2_{1,NO3} = \kappa^2_{NO3,1} \cdot \theta^{T-20}_{NO3} \tag{5-23}$$

$$\kappa_{2,NO3} = \kappa_{NO3,2} \cdot \theta^{T-20}_{NO3} \tag{5-24}$$

and the denitrification flux out of sediments as a nitrogen gas becomes:

$$J_{N2(g)} = \frac{\kappa^2_{1,NO3}}{s} NO3_1 + \kappa_{2,NO3} \cdot NO3_2 \tag{5-25}$$

$\kappa_{NO3,1}$ = reaction velocity for denitrification in Layer 1 at 20°C (m day^{-1})

$\kappa_{NO3,2}$ = reaction velocity for denitrification in Layer 2 at 20°C (m day^{-1})

θ_{NO3} = constant for temperature adjustment for $\kappa_{NO3,1}$ and $\kappa_{NO3,2}$

$J_{N2(g)}$ = denitrification flux (g N m^{-2} day^{-1})

$NO3_1$ = total nitrate nitrogen concentration in Layer 1 (g N m^{-3})

$NO3_2$ = total nitrate nitrogen concentration in Layer 2 (g N m^{-3}).

Once Equations 5-8 and 5-10 are solved for $NO3_1$ and $NO3_2$, the sediment flux of nitrate to the overlying water, $J_{aq,NO3}$, can be calculated using Eq. 5-9. The steady-state solution for nitrate showed that the nitrate flux is a linear function of $NO3_0$ (Eq. III-15 in D&F 1993): the intercept quantifies the amount of ammonium in the sediment that is nitrified but not denitrified (thus releases as $J_{aq,NO3}$), and the slope quantifies the extent to which overlying water nitrate is denitrified in the sediment. It also revealed that if the internal production of nitrate is small relative to the flux of nitrate from the overlying water, the normalized nitrate flux to the sediment, $- J_{aq,NO3}/NO3_0$, is linear in *s* for small *s* and constant for large *s*

(Section III-C in D&F 1993). For small *s* (~ 0.01 m day^{-1}), H_1 is large (Eq. 5-13) so that oxic layer denitrification predominates and $J_{aq,NO3}$ is essentially zero independent of $NO3_0$ (Fig. III-4 in D&F 1993).

5.3.4 Phosphate Phosphorus

Phosphate is produced by the diagenetic breakdown of POP in the lower layer:

$$J_{1,PO4} = 0 \qquad J_{2,PO4} = J_P \quad (from\ Eq.\ 5-7) \tag{5-26}$$

A portion of the liberated phosphate remains in the dissolved form and a portion becomes particulate phosphate, either via precipitation of phosphate-containing minerals (Troup 1974), e.g., vivianite, $Fe_3(PO_4)_2(s)$, or by partitioning to phosphate sorption sites (Lijklema 1980; Barrow 1983; Giordani and Astorri 1986). The extent of particulate formation is determined by the magnitude of the partition coefficients, $\pi_{1,PO4}$ and $\pi_{2,PO4}$, in Equations 5-11 and 5-12. Phosphate flux is strongly affected by DO_0, the overlying water oxygen concentration. As DO_0 approaches zero, the phosphate flux from the sediments increases. This mechanism is incorporated by making $\pi_{1,PO4}$ larger, under oxic conditions, than $\pi_{2,PO4}$. In the model, when DO_0 exceeds a critical concentration, $(DO_0)_{crit,PO4}$, sorption in the upper layer is enhanced by an amount $\Delta\pi_{PO4,1}$:

$$\pi_{1,PO4} = \pi_{2,PO4} \cdot (\Delta\pi_{PO4,1}) \qquad DO_0 > (DO_0)_{crit,PO4} \tag{5-27}$$

When oxygen falls below $(DO_0)_{crit,PO4}$, then:

$$\pi_{1,PO4} = \pi_{2,PO4} \cdot (\Delta\pi_{PO4,1})^{DO_0/(DO_0)_{crit,PO4}} \qquad DO_0 \leq (DO_0)_{crit,PO4} \tag{5-28}$$

which smoothly reduces $\pi_{1,PO4}$ to $\pi_{2,PO4}$ as DO_0 goes to zero. There is no removal reaction for phosphate in both layers:

$$\kappa_{1,PO4} = \kappa_{2,PO4} = 0 \tag{5-29}$$

Once Equations 5-8 and 5-10 are solved for $PO4_1$ and $PO4_2$, the sediment flux of phosphate to the overlying water, $J_{aq,PO4}$, can be calculated using Eq. 5-9.

5.3.5 Sulfide/Methane and Oxygen Demand

5.3.5.1 Sulfide. No diagenetic production of sulfide occurs in the upper layer. In the lower layer, sulfide is produced by carbon diagenesis (Eq. 5-7) decremented by the organic carbon consumed by denitrification (Eq. 5-25). Then:

$$J_{1,H2S} = 0 \qquad J_{2,H2S} = a_{O2,C} \cdot J_C - a_{O2,NO3} \cdot J_{N2(g)} \tag{5-30}$$

$a_{O2,C}$ = stoichiometric coefficient for carbon diagenesis consumed by sulfide oxidation (2.6667 g O_2-equivalents per g C)

$a_{O2,NO3}$ = stoichiometric coefficient for carbon diagenesis consumed by denitrification (2.8571 g O_2-equivalents per g N).

A portion of the dissolved sulfide that is produced in the anoxic layer reacts with the iron to form particulate iron monosulfide, FeS(s) (Morse et al. 1987). The particulate fraction is mixed into the oxic layer where it can be oxidized to ferric oxyhydroxide, Fe_2O_3(s). The remaining dissolved fraction also diffuses into the oxic layer where it is oxidized to sulfate. Partitioning between dissolved and particulate sulfide in the model represents the formation of FeS(s), which is parameterized using partition coefficients, $\pi_{1,H2S}$ and $\pi_{2,H2S}$, in Equations 5-11 and 5-12.

The present sediment model has three pathways for sulfide, the reduced end product of carbon diagenesis: (1) sulfide oxidation, (2) aqueous sulfide flux, and (3) burial. The distribution of sulfide among the three pathways is controlled by the partitioning coefficients and the oxidation reaction velocities (Section V-E in D&F 1993). Both dissolved and particulate sulfide are oxidized in the oxic layer, consuming oxygen in the process. In the oxic upper layer, the oxidation rate that is linear in oxygen concentration is used (Cline and Richards 1969; Millero 1986; Boudreau 1991). In the anoxic lower layer, no oxidation can occur. Then the reaction velocities in Equations 5-8 and 5-10 may be expressed as:

$$\kappa^2_{1,H2S} = \left(\kappa^2_{H2S,d1} \cdot fd_{1,H2S} + \kappa^2_{H2S,p1} \cdot fp_{1,H2S}\right) \theta^{T-20}_{H2S} \frac{DO_0}{2 \cdot KM_{H2S,O2}} \quad (5\text{-}31)$$

$$\kappa_{2,H2S} = 0 \quad (5\text{-}32)$$

$\kappa_{H2S,d1}$ = reaction velocity for dissolved sulfide oxidation in Layer 1 at 20°C (m day^{-1})

$\kappa_{H2S,p1}$ = reaction velocity for particulate sulfide oxidation in Layer 1 at 20°C (m day^{-1})

θ_{H2S} = constant for temperature adjustment for $\kappa_{H2S,d1}$ and $\kappa_{H2S,p1}$

$KM_{H2S,O2}$ = constant to normalize the sulfide oxidation rate for oxygen (g O_2 m^{-3}).

The constant, $KM_{H2S,O2}$, which is included for convenience only, is used to scale the oxygen concentration in the overlying water. At $DO_0 = KM_{H2S,O2}$, the reaction velocity for sulfide oxidation rate is at its nominal value.

The oxidation reactions in the oxic upper layer cause oxygen flux to the sediment, which exerts SOD. By convention, SOD is positive: $SOD = -J_{aq,O2}$. The SOD in the model consists of two components, carbonaceous sediment oxygen demand (CSOD) due to sulfide oxidation and nitrogenous sediment oxygen demand (NSOD) due to nitrification:

$$SOD = CSOD + NSOD = \frac{\kappa_{1,H2S}^2}{s} H2S_1 + a_{O2,NH4} \cdot J_{Nit} \quad (5\text{-}33)$$

$H2S_1$ = total sulfide concentration in Layer 1 (g O_2-equivalents m^{-3})

$a_{O2,NH4}$ = stoichiometric coefficient for oxygen consumed by nitrification (4.33 g O_2 per g N).

Equation 4-29 is nonlinear for SOD because the RHS contains *s* (= SOD/DO_0) so that SOD appears on both sides of the equation: note that J_{Nit} (Eq. 5-20) is also a function of *s*. A simple back substitution method is used, as explained in Section 5.6.1.

If the overlying water oxygen is low, then the sulfide that is not completely oxidized in the upper layer can diffuse into the overlying water. This aqueous sulfide flux out of the sediments, which contributes to the chemical oxygen demand in the water column model, is modeled using

$$J_{aq,H2S} = s(fd_{1,H2S} \cdot H2S_1 - COD) \quad (5\text{-}34)$$

The sulfide released from the sediment reacts very quickly in the water column when oxygen is available, but can accumulate in the water column under anoxic conditions. The COD, quantified as oxygen equivalents, is entirely supplied by benthic release in the water column model (Eq. 3-16). Since sulfide also is quantified as oxygen equivalents, COD is used as a measure of sulfide in the water column in Eq. 5-34.

5.3.5.2 Methane. When sulfate is used up, methane can be produced by carbon diagenesis and methane oxidation consumes oxygen (DiToro et al. 1990). Owing to the abundant sulfate in the saltwater, only the aforementioned sulfide production and oxidation are considered to occur in the saltwater. Since the sulfate concentration in fresh water is generally insignificant, methane production is considered to replace sulfide production in fresh water. In fresh water, methane is produced by carbon diagenesis in the lower layer decremented by the organic carbon consumed by denitrification, and no diagenetic production of methane occurs in the upper layer (Eq. 5-30):

$$J_{1,CH4} = 0 \qquad J_{2,CH4} = a_{O2,C} \cdot J_C - a_{O2,NO3} \cdot J_{N2(g)} \quad (5\text{-}35)$$

The dissolved methane produced takes two pathways: (1) oxidation in the oxic upper layer causing CSOD or (2) escape from the sediment as aqueous flux or as gas flux:

$$J_{2,CH4} = CSOD + J_{aq,CH4} + J_{CH4(g)} \quad (5\text{-}36)$$

$J_{aq,CH4}$ = aqueous methane flux (g O_2-equivalents m^{-2} day^{-1})

$J_{CH4(g)}$ = gaseous methane flux (g O_2-equivalents m^{-2} day^{-1}).

A portion of dissolved methane that is produced in the anoxic layer diffuses into the oxic layer where it is oxidized. This methane oxidation causes CSOD in the freshwater sediment (DiToro et al. 1990):

$$CSOD = CSOD_{\max} \cdot \left(1 - sech[\frac{\kappa_{CH4} \cdot \theta_{CH4}^{T-20}}{s}] \right) \quad (5\text{-}37)$$

$$CSOD_{\max} = minimum\{\sqrt{2 \cdot KL \cdot CH4_{sat} \cdot J_{2,CH4}},\ J_{2,CH4}\} \quad (5\text{-}38)$$

$$CH4_{sat} = 100\left(1 + \frac{h + H_2}{10} \right) 1.024^{20-T} \quad (5\text{-}39)$$

$CSOD_{max}$ = maximum CSOD occurring when all the dissolved methane transported to the oxic layer is oxidized

κ_{CH4} = reaction velocity for dissolved methane oxidation in Layer 1 at 20°C (m day^{-1})

θ_{CH4} = constant for temperature adjustment for κ_{CH4}

$CH4_{sat}$ = saturation concentration of methane in the pore water (g O_2-equivalents m^{-3}).

The term, $(h + H_2)/10$ where h and H_2 are in meters, in Eq. 5-39 is the depth from the water surface that corrects for the in situ pressure. Equation 5-39 is accurate to within 3% of the reported methane solubility between 5 and 20°C (Yamamoto et al. 1976).

If the overlying water oxygen is low, the methane that is not completely oxidized can escape the sediment into the overlying water either as aqueous flux or as gas flux. The aqueous methane flux, which contributes to the chemical oxygen demand in the water column model, is modeled using (DiToro et al. 1990):

$$J_{aq,CH4} = CSOD_{\max} \cdot sech[\frac{\kappa_{CH4} \cdot \theta_{CH4}^{T-20}}{s}] = CSOD_{\max} - CSOD \quad (5\text{-}40)$$

Methane is only slightly soluble in water. If its solubility, $CH4_{sat}$ given by Eq. 5-39, is exceeded in the pore water, it forms a gas phase that escapes as bubbles. The loss of methane as bubbles, i.e., the gaseous methane flux, is modeled using Eq. 5-36 with $J_{2,CH4}$ from Eq. 5-35, CSOD from Eq. 5-37, and $J_{aq,CH4}$ from Eq. 5-40 (DiToro et al. 1990).

5.4 Silica

The production of ammonium, nitrate, and phosphate in sediments is the result of the mineralization of POM by bacteria. The production of dissolved silica in sediments is the result of the dissolution of particulate biogenic or opaline silica, which is thought to be independent of bacterial processes.

The depositional flux of particulate biogenic silica from the overlying water to the sediments is modeled using Eq. 5-5. With this source, the mass-balance equation for particulate biogenic silica may be written as:

$$H_2 \frac{\partial PSi}{\partial t} = - S_{Si} \cdot H_2 - W \cdot PSi + J_{PSi} + J_{DSi} \quad (5\text{-}41)$$

PSi = concentration of particulate biogenic silica in the sediment (g Si m^{-3})

S_{Si} = dissolution rate of PSi in Layer 2 (g Si m^{-3} day^{-1})

J_{PSi} = depositional flux of PSi (g Si m^{-2} day^{-1}) given by Eq. 5-5

J_{DSi} = detrital flux of PSi (g Si m^{-2} day^{-1}) to account for PSi settling to the sediment that is not associated with the algal flux of biogenic silica.

The processes included in Eq. 5-41 are dissolution (i.e., production of dissolved silica), burial, and depositional and detrital fluxes from the overlying water. Equation 5-41 can be viewed as the analog of the diagenesis equations for POM (Eq. 5-6). The dissolution rate is formulated using a reversible reaction that is first order in silica solubility deficit and follows a Monod-type relationship in particulate silica:

$$S_{Si} = K_{Si} \cdot \theta_{Si}^{T-20} \frac{PSi}{PSi + KM_{PSi}} (Si_{sat} - fd_{2,Si} \cdot Si_2) \quad (5\text{-}42)$$

K_{Si} = first order dissolution rate for PSi at 20°C in Layer 2 (day^{-1})

θ_{Si} = constant for temperature adjustment for K_{Si}

KM_{PSi} = silica dissolution half-saturation constant for PSi (g Si m^{-3})

Si_{sat} = saturation concentration of silica in the pore water (g Si m^{-3}).

The mass-balance equations for mineralized silica can be formulated using the general forms, Equations 5-8 and 5-10. There is no source/sink term and no reaction in the upper layer:

$$J_{1,Si} = \kappa_{1,Si} = 0 \quad (5\text{-}43)$$

In the lower layer, silica is produced by the dissolution of particulate biogenic silica, which is modeled using Eq. 5-42. The two terms in Eq. 5-42 correspond to the source term and reaction term in Eq. 5-10:

$$J_{2,Si} = K_{Si} \cdot \theta_{Si}^{T-20} \frac{PSi}{PSi + KM_{PSi}} Si_{sat} \cdot H_2 \quad (5\text{-}44)$$

$$\kappa_{2,Si} = K_{Si} \cdot \theta_{Si}^{T-20} \frac{PSi}{PSi + KM_{PSi}} f_{d2,Si} \cdot H_2 \quad (5\text{-}45)$$

A portion of silica dissolved from particulate silica sorbs to solids and a portion remains in the dissolved form. Partitioning using the partition coefficients, $\pi_{1,Si}$ and $\pi_{2,Si}$, in Equations 5-11 and 5-12 controls the

extent to which dissolved silica sorbs to solids. Since silica shows similar behavior as phosphate in the adsorption-desorption process, the same partitioning method as applied to phosphate (Section 5.3.4) is used for silica. That is, when DO_0 exceeds a critical concentration, $(DO_0)_{crit,Si}$, sorption in the upper layer is enhanced by an amount $\Delta\pi_{Si,1}$:

$$\pi_{1,Si} = \pi_{2,Si} \cdot (\Delta\pi_{Si,1}) \qquad DO_0 > (DO_0)_{crit,Si} \tag{5-46}$$

When oxygen falls below $(DO_0)_{crit,Si}$, then:

$$\pi_{1,Si} = \pi_{2,Si} \cdot (\Delta\pi_{Si,1})^{DO_0/(DO_0)_{crit,Si}} \qquad DO_0 \leq (DO_0)_{crit,Si} \tag{5-47}$$

which smoothly reduces $\pi_{1,Si}$ to $\pi_{2,Si}$ as DO_0 goes to zero.

Once Equations 5-8 and 5-10 are solved for Si_1 and Si_2, the sediment flux of silica to the overlying water, $J_{aq,Si}$, can be calculated using Eq. 5-9.

5.5 Sediment Temperature

All rate coefficients in the aforementioned mass-balance equations are expressed as a function of sediment temperature, T. The sediment temperature is modeled based on the diffusion of heat between the water column and sediment:

$$\frac{\partial T}{\partial t} = \frac{D_T}{H^2}(T_W - T) \tag{5-48}$$

D_T = heat diffusion coefficient between the water column and sediment (m^2 sec^{-1})

T_W = temperature in the overlying water column (°C) calculated by Eq. 4-82.

The model application in D&F and Cerco and Cole (1993) used $D_T = 1.8 \times 10^{-7}$ m^2 sec^{-1}.

5.6 Method of Solution

5.6.1 Finite-Difference Equations and Solution Scheme

An implicit integration scheme is used to solve the governing mass-balance equations. The finite difference form of Eq. 5-8 may be expressed as:

$$0 = s(fd_0 \cdot Ct_0' - fd_1 \cdot Ct_1') + KL(fd_2 \cdot Ct_2' - fd_1 \cdot Ct_1') + \omega(fp_2 \cdot Ct_2' - fp_1 \cdot Ct_1')$$

$$- W \cdot Ct_1' - \frac{\kappa_1^2}{s} Ct_1' + J_1' \tag{5-49}$$

where the primed variables designate the values evaluated at $t+\theta$ and the unprimed variables are those at t, where θ is defined in Eq. 4-82. The finite difference form of Eq. 5-10 may be expressed as:

$$0 = -KL(fd_2 \cdot Ct_2' - fd_1 \cdot Ct_1') - \omega(fp_2 \cdot Ct_2' - fp_1 \cdot Ct_1') + W(Ct_1' - Ct_2') - (\kappa_2 + \frac{H_2}{\theta})Ct_2' + \left(J_2' + \frac{H_2}{\theta}Ct_2\right) \quad (5\text{-}50)$$

The two terms, $-(H_2/\theta)Ct_2'$ and $(H_2/\theta)Ct_2$, are from the derivative term, $H_2(\partial Ct_2/\partial t)$ in Eq. 5-10, each of which simply adds to the Layer 2 removal rate and the forcing function, respectively. Setting these two terms equal to zero results in the steady-state model. The two unknowns, Ct_1' and Ct_2', can be calculated at every time step using:

$$\begin{pmatrix} s \cdot fd_1 + a_1 + \frac{\kappa_1^2}{s} & -a_2 \\ -a_1 & a_2 + W + \kappa_2 + \frac{H_2}{\theta} \end{pmatrix} \begin{pmatrix} Ct_1' \\ Ct_2' \end{pmatrix} = \begin{pmatrix} J_1' + s \cdot fd_0 \cdot Ct_0' \\ J_2' + \frac{H_2}{\theta}Ct_2 \end{pmatrix} \quad (5\text{-}51)$$

$$a_1 = KL \cdot fd_1 + \omega \cdot fp_1 + W \qquad a_2 = KL \cdot fd_2 + \omega \cdot fp_2 \quad (5\text{-}52)$$

The solution of Eq. 5-51 requires an iterative method since the surface mass transfer coefficient, s, is a function of the SOD (Eq. 5-13), which is also a function of s (Eq. 5-33). A simple back substitution method is used:

(1) Start with an initial estimate of SOD: for example, SOD = $a_{O2,C} \cdot J_C$ or the previous time step SOD.
(2) Solve Eq. 5-51 for ammonium, nitrate, and sulfide/methane.
(3) Compute the SOD using Eq. 5-33.
(4) Refine the estimate of SOD: a root finding method (Brent's method in Press et al. 1986) is used to make the new estimate.
(5) Go to (2) if no convergence.
(6) Solve Eq. 5-51 for phosphate and silica.

For the sake of symmetry, the equations for diagenesis, particulate biogenic silica and sediment temperature are also solved in implicit form. The finite difference form of the diagenesis equation (Eq. 5-6) may be expressed as:

$$G_{POM,i}' = \left(G_{POM,i} + \frac{\theta}{H_2}J_{POM,I}\right)\left(1 + \theta \cdot K_{POM,i} \cdot \theta_{POM,i}^{T-20} + \frac{\theta}{H_2}W\right)^{-1} \quad (5\text{-}53)$$

The finite difference form of the PSi equation (Eq. 5-41) may be expressed as:

$$PSi' = \left(PSi + \frac{\theta}{H_2}(J_{PSi} + J_{DSi}) \right) \left(1 + \theta \cdot K_{Si} \cdot \theta_{Si}^{T-20} \frac{Si_{sat} - f_{d2,Si} \cdot Si_2}{PSi + KM_{PSi}} + \frac{\theta}{H_2} W \right)^{-1} \quad (5\text{-}54)$$

using Eq. 5-36 for the dissolution term, in which PSi in the Monod-type term has been kept at time level *t* to simplify the solution. The finite difference form of the sediment temperature equation (Eq. 5-48) may be expressed as:

$$T' = \left(T + \frac{\theta}{H^2} D_T \cdot T_W \right) \left(1 + \frac{\theta}{H^2} D_T \right)^{-1} \quad (5\text{-}55)$$

5.6.2 Boundary and Initial Conditions

The above finite difference equations constitute an initial boundary-value problem. The boundary conditions are the depositional fluxes ($J_{POM,i}$ and J_{PSi}) and the overlying water conditions (Ct_0 and T_W) as a function of time, which are provided from the water column water quality model. The initial conditions are the concentrations at $t = 0$, $G_{POM,i}(0)$, PSi(0), $Ct_1(0)$, $Ct_2(0)$, and T(0), to start the computations. Strictly speaking, these initial conditions should reflect the past history of the overlying water conditions and depositional fluxes, which is often impractical because of lack of field data for these earlier years.